STEADY-STATE POWER FLOW ANALYSIS OF ELECTRICAL POWER SYSTEMS MODELLED BY 2-DIMENSIONAL MULTIBOND GRAPHS

Israel Núñez-Hernández[(a)], Peter C. Breedveld[(b)], Paul B. T. Weustink[(c)], Gilberto Gonzalez-A[(d)]

[(a),(b)] Robotics and Mechatronics Group, University of Twente, Enschede, Netherlands
[(c)] Controllab Products B.V, Hengelosestraat 500, 7521 AN Enschede, Netherlands
[(d)] Faculty of Electrical Engineering, University of Michoacan, Morelia, Michoacán, Mexico

[(a)] i.nunezhernandez@utwente.nl, [(b)] p.c.breedveld@utwente.nl
[(c)] paul.weustink@controllab.nl, [(d)] gilmichga@yahoo.com.mx

ABSTRACT
The steady-state analysis of electrical circuits is frequently done by means of phasors. This paper focuses on the use of multiport elements with two-dimensional multibond as representation of the real and imaginary part of a phasor. This set of two-dimensional multibonds forms, together with elements that are adapted likewise, a so-called phasor bond graph model. A procedure is presented to derive a symbolic function of the steady-state of a user-defined output from a phasor bond graph model. The application of a phasor bond graph model in power flow studies of an electrical power system are presented as an example.

Keywords: steady-state; power flow; phasor; bond graph, electrical power systems

1. INTRODUCTION

An electrical power system (EPS) consists of many individual elements connected together to form a large, complex and dynamic system capable of generating, transmitting and distributing electrical energy over a large geographical area (Machowski et al., 2008).
Power system stability (PSS) may be defined as the ability to retrieve an equilibrium state of such a system after being subjected to a physical disturbance. Three quantities are important for power system operation: i) phase-angles of nodal voltages, also called power or load angles; ii) frequency; and iii) nodal voltage magnitude (Machowski et al., 2008; Kundur, 1994).
In the stability analysis of practical power systems consisting of thousands of buses and hundreds of generators. It is common to assume all machines to be in a steady-state condition prior to a disturbance (Kundur, 1994; Anderson and Fouad, 2003).
The sinusoidal analysis by means of phasors is an elegant way to analyze electrical circuits with sinusoidal inputs and responses with a given constant frequency, i.e. when the system is in steady-state, without the need to solve differential equations (Steinmetz, 1893).
At the other hand, bond graph (BG) methodology deals with a graphical approach to system modelling, the essential feature of the bond graph approach is the concise representation of energy storage, dissipation, and exchange in a system. It describes how the power flows through the system. The overall purpose of this methodology is the domain-independent representation of any engineering system which is involved in different domains (Paynter, 1961).
Previous studies have reported how steady-state values can be obtained from BG models of dynamic systems. An algorithm to determine the equilibrium state of a system with constant inputs by direct inspection of its BG is proposed in (Breedveld, 1984a). A BG model in a derivative causality assignment is proposed to determine the steady-state of a linear system in (Gonzalez-A, 2003). However, the previously mentioned approaches are mainly focus on the final amplitude value of the defined output. They do not give in a direct manner information about the phase shift of the signals. As mentioned above, for the case of EPS, the phase-angle of a nodal voltage is important since the power flow depends on it.
This paper attempts to show the use of phasors together with bond graphs by means of two-dimensional (2D) multibonds. The main issues addressed in this paper are: i) the formulation of regular BG elements into phasor bond graph (PhBG) elements; ii) the procedure to obtain a symbolic function in the complex plane of a given output; and iii) the power flow analysis of EPS's.
The paper has been organized in the following way. In order to inform the reader about phasor theory and BG methodology, Section 2 and Section 3 respectively present a brief background of these topics, including references for further reading. If the reader has previous knowledge of the topics these sections can be skipped without any trouble. Section 4 presents the theoretical background to obtain the PhBG elements. In Section 5, the methodology proposed to determine a symbolic function of the steady-state from a PhBG model is described. Furthermore, the proposed methodology is applied to a passive band pass filter in order to obtain a symbolic function of its steady state as an example. Section 6 addresses the application of PhBG to the analysis of power flow of a simple EPS. Finally, the conclusions are stated in Section 7.

2. PHASOR REPRESENTATION

2.1. Introduction

A phasor represents a periodic waveform as a "rotary vector". This is illustrated in Fig. 1. Suppose a vector **F** rotating with angular velocity ω with respect to a stationary reference frame. Its position at any instant of time is given by $\mathbf{F}(t) = \hat{A}e^{j(\omega t+\theta)}$, where $\hat{A}$ is the amplitude and θ is the phase shift with respect to the reference frame Re-Im. The projection of vector **F** onto the fixed horizontal axis is a sinusoidal function expressed as $f(t) = \hat{A}\cos(\omega t + \theta)$.

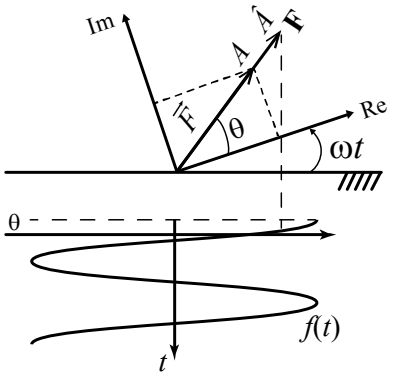

Fig. 1 Illustration of definition of phasors

The amplitude $\hat{A}$ may be expressed in rms value, A. For sinusoidal waves $\hat{A} = \sqrt{2}A$. Then, it is possible rewrite the vector position in the following way:

$$\mathbf{F}(t) = \sqrt{2}Ae^{j\theta}e^{j\omega t} \tag{1}$$

The part that does not depend on time $Ae^{j\theta}$ in (1) is known as a phasor (Veltman, 2007). A phasor $\vec{F}$ may also be written as,

$$\vec{F} = Ae^{j\theta} = A\angle\theta = A(\cos\theta + j\sin\theta) \tag{2}$$

The time integral and time derivative of ***F***(*t*) are

$$\begin{aligned}\int \mathbf{F}(t)dt &= \sqrt{2}Ae^{j\theta}\int e^{j\omega t}dt = -j\tfrac{1}{\omega}\sqrt{2}\vec{F}e^{j\omega t}\\ \tfrac{d}{dt}\mathbf{F}(t) &= \sqrt{2}Ae^{j\theta}\tfrac{d}{dt}e^{j\omega t} = j\omega\sqrt{2}\vec{F}e^{j\omega t}\end{aligned} \tag{3}$$

which implies that the integral of the phasor is lagged by π/2 radians, and scaled by 1/ω. At the other hand, the derivative of a phasor is leaded by $\pi/2$ radians, and multiplied by ω. This means that in phasor notation the integration and differentiation operations can be performed by scaling and phase shifting.

2.2. Analysis of Electrical Networks with Phasors

Phasors are an efficient method for steady-state analysis of AC circuits with a given constant frequency. When the system operates in a steady-state condition, differential equations are not necessary since all variables are either constants or sinusoidal variations with time. With these terms neglected, equations appear as algebraic equations. In an electrical network, let the instantaneous voltage and the instantaneous current be

$$\begin{aligned}v(t) &= v\cos(\omega t + \theta_v)\\ i(t) &= i\cos(\omega t + \theta_i)\end{aligned} \tag{4}$$

The phasor representation of (4) may be obtained by using (1) and (2), thus

$$\begin{aligned}\vec{V} &= Ve^{j\theta_v} = V\angle\theta_v\\ \vec{I} &= Ie^{j\theta_i} = I\angle\theta_i\end{aligned} \tag{5}$$

The impedance, *Z*, is the relationship between the voltage and current. Since this relationship is between two phasors, it will be a phasor too. The impedance may be expressed as

$$\vec{Z} = \vec{V}/\vec{I} = Z\angle\theta = R + j\left(X_L - X_C\right) \tag{6}$$

where $\theta = \theta_v - \theta_i$ is called the impedance angle. The real part is given by the resistive elements *R*, and the imaginary or reactive part, is given by the inductive and capacitive reactances in the system, respectively X_L and X_C. Table 1 shows a list of the three basic elements (resistor, inductor, and capacitor) in an electrical network and their impedances.

Table 1: Impedances

Time	Phasor	Impedance
$v(t) = R\cdot i(t)$	$\vec{V} = R\cdot\vec{I}$	R
$v(t) = L\frac{d}{dt}i(t)$	$\vec{V} = jX_L\vec{I}$	$jX_L = j\omega L$
$v(t) = \frac{1}{C}\cdot\int i(t)\,dt$	$\vec{V} = -jX_C\vec{I}$	$-jX_C = 1/j\omega C$

In power engineering, voltages, and currents are often represented in a phasor diagram. A phasor diagram is a "picture" at any instant of these rotary vectors, which represents the phase relationship between them at that time.

2.3. Complex Power

The instantaneous power consumed by the network may be written as,

$$\begin{aligned}p(t) &= v(t)\cdot i(t) = v\cdot i\cos(\omega t + \theta_v)\cos(\omega t + \theta_i)\\ &= P(1 + \cos 2(\omega t + \theta_v)) + Q\sin 2(\omega t + \theta_v)\end{aligned} \tag{7}$$

with $P = VI\cos\theta$, $Q = VI\sin\theta$, and $\theta = \theta_v - \theta_i$. The variable *P* is called real or *active power* defined in watts (*W*). It represents the absorbed power by the resistive elements in the load. At the other hand, *Q* is referred as *reactive power*, defined in volt-ampere reactive (*var*), and this power supplies the stored energy in reactive elements. Since cosθ plays an important role in the

ISBN 978-88-97999-63-8; Bruzzone, Dauphin-Tanguy, Junco and Longo Eds.

amount of real power in the system, it is called *power factor* (Saadat, 1999; El-Hawary, 1995).
Real, and reactive power are represented together as a complex or *apparent power*, *S*, its unit is volt-ampere (*VA*) (Chapman, 2005). The apparent power may be represented as,

$$\begin{aligned}\vec{S} &= P + jQ = \vec{V}\vec{I}^{*} = \vec{Z}\,|\vec{I}\,| \\ &= R\,|\vec{I}\,|^{2} + jX\,|\vec{I}\,|^{2} \\ &= (V_{\mathrm{Re}}I_{\mathrm{Re}} + V_{\mathrm{Im}}I_{\mathrm{Im}}) + j(V_{\mathrm{Im}}I_{\mathrm{Re}} - V_{\mathrm{Re}}I_{\mathrm{Im}})\end{aligned} \tag{8}$$

where $\vec{I}^{*}$ is the conjugate current. These three powers are normally described in a so-called power triangle.

3. BOND GRAPHS

The port-based approach with regard to modeling of physical systems is an effective way to split a system model into conceptual elements that are interacting with each other via (power) ports. As it is based on energy, port-based modelling offers a unified way to model physical systems from different physical domains, such as electrical, magnetic, mechanical, hydraulic, thermal, etc.
A BG is a graphical notation of such a port-based description. The BG conceptual framework was originated by Paynter in (Paynter, 1961).
This graphical technique is based on representing power transfer between elements as labelled nodes, which are linked to each other by means of oriented edges called *bonds*. In each physical domain, the power can be written as the product of two variables, *effort* $e(t)$ and *flow* $f(t)$. This pair of variables is called *power variables*. Conserved physical variables can either be the time integral of a flow (generalized *displacement* $q(t)$) or the time integral of an effort (generalized *momentum* $p(t)$) and can be considered as stored quantities, *state variables* or *energy variables*, as the stored energy is a function of these variables. By making the distinction between displacement-like states and momentum-like states, the mechanical framework of variables is used as opposed to the more general, but less known, generalized framework of variables (Breedveld, 1984b).
In a bond graph, the way in which these variables need to be computed are specified as input and output to the constitutive relation that characterizes a port is indicated by means of a so-called causal stroke. It is a perpendicular line put at one end of a bond indicating the direction of the effort signal, also called the causality.
The port-based approach is in principle an object-oriented approach to modeling. This permits different realizations of an object by directly replacing a portion of it with another bond graph system with a different degree of dynamic details.
The basic elements (nodes) of the bond graph language can be classified as follows:

- 1-port elements, which dissipate (free) energy (resistor *R*), store energy (inertia *I*, capacitor *C*) and supply power (sources S_e, S_f).
- 2-port elements (transformers TF and gyrators GY) are used when it is necessary to interconnect submodels in different domains in a power conservative way. However, transformers can also be used for scaling variables in a power conserving manner.
- Multiport elements that represent the conceptual structure of the model. The 0-junction is a BG node with common effort; the 1-junction describes a common flow node.

A BG model can be organized into interconnected blocks (modulated sources, storage block, dissipation block, junction structure, ideal sensors). It is possible to obtain the state-space equations of the system using a BG model. Fig. 2 shows a multiport linear time-invariant (LTI) system, which includes the key vectors of BG variables by the input-output role they play in the causal problem (Rosenberg, 1971).

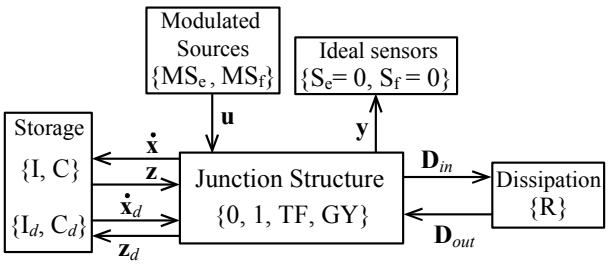

Fig. 2 Block representation and key vectors of a bond graph model

In Fig. 2, the state vector $\mathbf{x} \in \Re^{n}$ is composed of generalized state variables; $\mathbf{z} \in \Re^{n}$, the vector of power variables (C-port efforts and I-port flows); $\mathbf{u} \in \Re^{p}$ denotes the vector of system input variables; $\mathbf{D}_{in} \in \Re^{r}$, and $\mathbf{D}_{out} \in \Re^{r}$ contain mixed sets of efforts and flows and their inner product represent the energy exchange between the dissipation multiport and the junction structure; $\mathbf{x}_d \in \Re^{q}$ is the state vector associated with elements in derivative causality; $\mathbf{z}_d \in \Re^{q}$, the vector of power variables in derivative causality (I-port efforts and C-port flows); finally, the vector $\mathbf{y} \in \Re^{k}$ is the system output variables. The outputs can be measured by means of ideal sensors. As the amount of power the ideal sensors take out of the system is zero, then the device can be modelled by an energy sink that provides a zero effort or a zero flow. As a result, an effort sensor can be represented by a zero flow sink and a flow sensor can be modelled by a zero effort sink.
The storage and dissipation block relationships are,

$$\mathbf{z} = \mathbf{F}\mathbf{x}; \quad \mathbf{z}_d = \mathbf{F}_d\,\mathbf{x}_d; \quad \mathbf{D}_{out} = \mathbf{L}\mathbf{D}_{in} \tag{9}$$

where $\mathbf{F}$ is a diagonal matrix composed of the elements in integral causality, $\mathbf{F}_d$ is a diagonal matrix composed of the elements in derivative causality, and $\mathbf{L}$ is a diagonal matrix composed of the dissipative elements.

The junction structure matrix deduced from Fig. 2 has the following form:

$$\begin{bmatrix} \dot{\mathbf{x}} \\ \mathbf{D}_{in} \\ \mathbf{y} \\ \mathbf{z}_d \end{bmatrix} = \begin{bmatrix} \mathbf{S}_{11} & \mathbf{S}_{12} & \mathbf{S}_{13} & \mathbf{S}_{14} \\ \mathbf{S}_{21} & \mathbf{S}_{22} & \mathbf{S}_{23} & \mathbf{0} \\ \mathbf{S}_{31} & \mathbf{S}_{32} & \mathbf{S}_{33} & \mathbf{0} \\ \mathbf{S}_{41} & \mathbf{0} & \mathbf{0} & \mathbf{0} \end{bmatrix} \begin{bmatrix} \mathbf{z} \\ \mathbf{D}_{out} \\ \mathbf{u} \\ \dot{\mathbf{x}}_d \end{bmatrix} \tag{10}$$

Because of some usual hypotheses the matrix **S**, satifies the following properties (Karnopp et al., 1990; Rosenberg, 1971):

- no connection between the dissipation block and elements in derivative causality: $\mathbf{S}_{24} = \mathbf{S}_{42} = \mathbf{0}$,
- no connection between the sources/sensors and the elements in derivative causality: $\mathbf{S}_{34} = \mathbf{S}_{43} = \mathbf{0}$,
- $\mathbf{S}_{11}$ and $\mathbf{S}_{22}$ are square skew-symmetric matrices
- if there is no causal connection between dissipative elements, then: $\mathbf{S}_{22} = \mathbf{0}$,
- causal connection between elements with integral and derivative causality: $\mathbf{S}_{14} = -\mathbf{S}_{41}{}^{T}$,
- $\mathbf{S}_{12}$ and $\mathbf{S}_{21}$ are each other's negative transpose.

The entries of the **S** matrix take values inside the set $\{0, \pm 1, \pm m, \pm n\}$, where *m,* and *n* are transformer, and gyrator modules. Conveniently representing the state equations as

$$\begin{aligned} \dot{\mathbf{x}} &= \mathbf{A}\,\mathbf{x} + \mathbf{B}\,\mathbf{u} \\ \mathbf{y} &= \mathbf{C}\,\mathbf{x} + \mathbf{D}\,\mathbf{u} \end{aligned} \tag{11}$$

where

$$\begin{aligned} \mathbf{A} &= \mathbf{E}^{-1}(\mathbf{S}_{11} + \mathbf{S}_{12}\mathbf{M}\,\mathbf{S}_{21})\mathbf{F} \\ \mathbf{B} &= \mathbf{E}^{-1}(\mathbf{S}_{13} + \mathbf{S}_{12}\mathbf{M}\,\mathbf{S}_{23}) \\ \mathbf{C} &= (\mathbf{S}_{31} + \mathbf{S}_{32}\mathbf{M}\,\mathbf{S}_{21})\mathbf{F} \\ \mathbf{D} &= \mathbf{S}_{33} + \mathbf{S}_{32}\mathbf{M}\,\mathbf{S}_{23} \end{aligned} \tag{12}$$

being $\mathbf{M} = (\mathbf{I} - \mathbf{L}\,\mathbf{S}_{22})^{-1}\mathbf{L}$, $\mathbf{E} = \mathbf{I} + \mathbf{S}_{14}\mathbf{F}_d{}^{-1}\mathbf{S}_{14}{}^{T}\mathbf{F}$, and $\mathbf{I}$ the identity matrix of appropriate dimension. The reader interested in more details about BG, may refer to (Karnopp et al., 1990; Borutzky, 2010).

4. PHASOR BOND GRAPHS ELEMENTS

The Laplace transform can also be applied to the BG models (Borutzky, 2010; Kypuros, 2013). With this transformation, the regular passive BG elements become impedances, or admittances.

As shown in Fig. 3*a*), if a 1-port element has effort-out causality can be characterized by an impedance, while a 1-port element with flow-out causality is modelled as an admittance, see Fig. 3*b*). In order to represent dynamic systems using impedances, it must be assumed that the constitutive relationships of the components are linear.

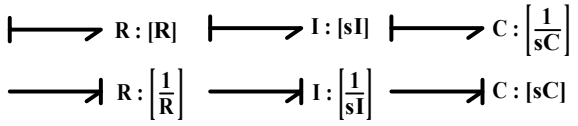

Fig. 3 1-port elements *a*) impedances, and *b*) admittances

Impedance bond graphs are synthesized by following the same procedure that in the case of dynamic models. If the Laplace operator is substituted by the Fourier operator, i.e. $s = j\omega$, the PhBG elements may be obtained. Thus, an impedance BG model becomes a PhBG model.

The proposed PhBG model expresses the impedances in matrix form. In this way, the phasor elements may be represented using 2D multibonds (Bonderson, 1975; Breedveld, 1985). While one bond represents the real part of the phasor, the second bond represents the imaginary part of the phasor. The impedances from Table 1 are rewritten in matrix form, see Table 2.

Table 2: 1-Port Impedances in Phasor Bond Graph Form

Element	Phasor	2D multibond
Resistive	$\begin{bmatrix} V_{\mathrm{Re}} \\ V_{\mathrm{Im}} \end{bmatrix} = R \begin{bmatrix} 1 & 0 \\ 0 & 1 \end{bmatrix} \begin{bmatrix} I_{\mathrm{Re}} \\ I_{\mathrm{Im}} \end{bmatrix}$	⟹ **R**
Inductive	$\begin{bmatrix} V_{\mathrm{Re}} \\ V_{\mathrm{Im}} \end{bmatrix} = X_L \begin{bmatrix} 0 & -1 \\ 1 & 0 \end{bmatrix} \begin{bmatrix} I_{\mathrm{Re}} \\ I_{\mathrm{Im}} \end{bmatrix}$	⟹ $\mathbf{X_L}$
Capacitive	$\begin{bmatrix} V_{\mathrm{Re}} \\ V_{\mathrm{Im}} \end{bmatrix} = X_C \begin{bmatrix} 0 & 1 \\ -1 & 0 \end{bmatrix} \begin{bmatrix} I_{\mathrm{Re}} \\ I_{\mathrm{Im}} \end{bmatrix}$	⟹ $\mathbf{X_C}$

The 2-port elements are modelled in the same way as in case of 2D multibonds (Breedveld, 1985), see Table 3.

Table 3: 2-Port Elements in Phasor Bond Graph Form

Element	Phasor	2D multibond
Transformer	$\begin{bmatrix} \vec{V}_1 \\ \vec{I}_2 \end{bmatrix} = \begin{bmatrix} 0 & \mathbf{T}^T \\ \mathbf{T} & 0 \end{bmatrix} \begin{bmatrix} \vec{I}_1 \\ \vec{V}_2 \end{bmatrix}$; $\mathbf{T} = \begin{bmatrix} m & 0 \\ 0 & m \end{bmatrix}$	⟹ **TF** ⟹
Gyrator	$\begin{bmatrix} \vec{V}_1 \\ \vec{I}_2 \end{bmatrix} = \begin{bmatrix} 0 & \mathbf{G}^T \\ \mathbf{G} & 0 \end{bmatrix} \begin{bmatrix} \vec{I}_1 \\ \vec{V}_2 \end{bmatrix}$; $\mathbf{G} = \begin{bmatrix} n & 0 \\ 0 & n \end{bmatrix}$	⟹ **GY** ⟹

m and *n* are the scalar modulus of the transformer and gyrator, respectively

The 2D multibond sources from (5) can be changed into its matrix form using (2). See Table 4.

Table 4: Sources in Phasor Bond Graph Form

Source	Phasor	2D multibond
Voltage	$\vec{V} = V[\cos\theta_v \quad \sin\theta_v]^T$	$\mathbf{V}\angle\theta$ ⟹
Current	$\vec{I} = I[\cos\theta_i \quad \sin\theta_i]^T$	$\mathbf{I}\angle\theta$ ⟹

V and *I* are the rms value of voltage and current, respectively

5. PHASOR BOND GRAPH ANALYSIS

This section presents the analysis required to obtain a symbolic function from a PhBG model that represents the steady-state of user-defined output. In a PhBG model there is not difference between elements in integral or derivative causality, since they are replaced by their equivalent admittance or impedance. In other words, a PhBG model only contains passive elements with indifferent causality. Nevertheless, in order to maintain the familiarity between regular BG and PhBG models, the Standard Causality Assignment Procedure (SCAP) introduced in (Karnopp and Rosenberg, 1968) is applied to the PhBG models. Similar to the regular BG analysis. The block representation of a PhBG is depicted in Fig. 4.

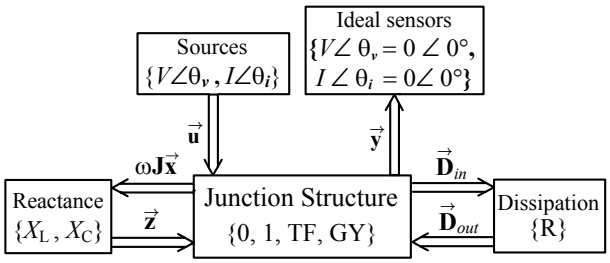

Fig. 4 Block representation of a phasor bond graph model

The reactance, and dissipation blocks contain the power demanding elements of the system, and may be defined as

$$\vec{\mathbf{z}} = \vec{\mathbf{F}}(\omega\mathbf{J}\vec{\mathbf{x}}); \qquad \vec{\mathbf{D}}_{out} = \vec{\mathbf{L}}\,\vec{\mathbf{D}}_{in} \tag{13}$$

where

$$\mathbf{J} = \begin{bmatrix} 0 & -1 \\ 1 & 0 \end{bmatrix} \tag{14}$$

and $\vec{\mathbf{F}}$ is a diagonal matrix filled with the impedance, or admittance of the reactive elements. The diagonal matrix $\vec{\mathbf{L}}$ contains the impedance, or admittance of the resistive elements.

The junction structure relationships of a PhBG model can be defined as follows:

$$\begin{bmatrix} \omega\mathbf{J}\vec{\mathbf{x}} \\ \vec{\mathbf{D}}_{in} \\ \vec{\mathbf{y}} \end{bmatrix} = \begin{bmatrix} \vec{\mathbf{S}}_{11} & \vec{\mathbf{S}}_{12} & \vec{\mathbf{S}}_{13} \\ \vec{\mathbf{S}}_{21} & \vec{\mathbf{S}}_{22} & \vec{\mathbf{S}}_{23} \\ \vec{\mathbf{S}}_{31} & \vec{\mathbf{S}}_{32} & \vec{\mathbf{S}}_{33} \end{bmatrix} \begin{bmatrix} \vec{\mathbf{z}} \\ \vec{\mathbf{D}}_{out} \\ \vec{\mathbf{u}} \end{bmatrix} \tag{15}$$

After some algebraic manipulations, the system output is given by

$$\vec{\mathbf{y}} = (\vec{\mathbf{C}}(\vec{\mathbf{F}}^{-1} - \vec{\mathbf{A}})^{-1}\vec{\mathbf{B}} + \vec{\mathbf{D}})\,\vec{\mathbf{u}} \tag{16}$$

with

$$\begin{aligned} \vec{\mathbf{A}} &= \vec{\mathbf{S}}_{11} + \vec{\mathbf{S}}_{12}\vec{\mathbf{M}}\vec{\mathbf{S}}_{21} \\ \vec{\mathbf{B}} &= \vec{\mathbf{S}}_{13} + \vec{\mathbf{S}}_{12}\vec{\mathbf{M}}\vec{\mathbf{S}}_{23} \\ \vec{\mathbf{C}} &= \vec{\mathbf{S}}_{31} + \vec{\mathbf{S}}_{32}\vec{\mathbf{M}}\vec{\mathbf{S}}_{21} \\ \vec{\mathbf{D}} &= \vec{\mathbf{S}}_{33} + \vec{\mathbf{S}}_{32}\vec{\mathbf{M}}\vec{\mathbf{S}}_{23} \end{aligned} \tag{17}$$

being $\vec{\mathbf{M}} = (\mathbf{I} - \vec{\mathbf{L}}\vec{\mathbf{S}}_{22})^{-1}\vec{\mathbf{L}}$, and $\mathbf{I}$ the identity matrix of appropriate dimension.

5.1. Example: Passive Filter

To clarify the application of the PhBG analysis, it will be shown an example. Consider the passive band pass circuit depicted in Fig. 5*a*).

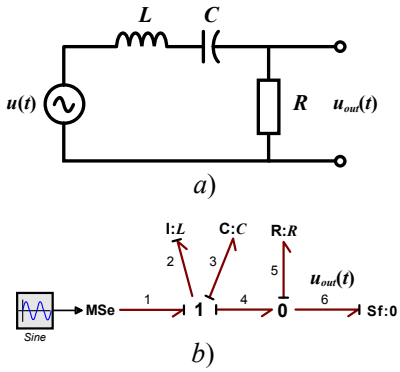

Fig. 5 Passive band pass filter

In Fig. 5*b*) is possible to observe the BG model of the filter. As illustrated in Fig. 6, the BG model was changed into a PhBG model by using the 2D multibonds, the SCAP and the impedance/admittance of each element.

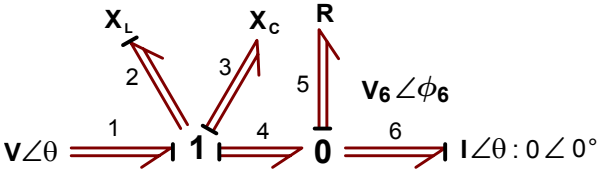

Fig. 6 PhBG model of the band pass filter

The key vectors obtained from the PhBG model are,

$$\begin{aligned} \omega\mathbf{J}\vec{\mathbf{x}} &= \begin{bmatrix} \vec{e}_2 \\ \vec{f}_3 \end{bmatrix} = \begin{bmatrix} e_{2\,\mathrm{Re}} \\ e_{2\,\mathrm{Im}} \\ f_{3\,\mathrm{Re}} \\ f_{3\,\mathrm{Im}} \end{bmatrix}; \quad \vec{\mathbf{z}} = \begin{bmatrix} \vec{f}_2 \\ \vec{e}_3 \end{bmatrix} = \begin{bmatrix} f_{2\,\mathrm{Re}} \\ f_{2\,\mathrm{Im}} \\ e_{3\,\mathrm{Re}} \\ e_{3\,\mathrm{Im}} \end{bmatrix} \\ \vec{\mathbf{D}}_{in} &= \vec{f}_5 = \begin{bmatrix} f_{5\,\mathrm{Re}} \\ f_{5\,\mathrm{Im}} \end{bmatrix}; \quad \vec{\mathbf{D}}_{out} = \vec{e}_5 = \begin{bmatrix} e_{5\,\mathrm{Re}} \\ e_{5\,\mathrm{Im}} \end{bmatrix} \\ \vec{\mathbf{u}} &= \vec{e}_1 = \begin{bmatrix} e_{1\,\mathrm{Re}} \\ e_{1\,\mathrm{Im}} \end{bmatrix}; \quad \vec{\mathbf{y}} = \vec{e}_6 = \begin{bmatrix} e_{6\,\mathrm{Re}} \\ e_{6\,\mathrm{Im}} \end{bmatrix} \end{aligned} \tag{18}$$

Note that in (18) the chosen output is the voltage difference over the resistor. The constitutive relations of the 2D multibond elements are

$$\vec{\mathbf{F}} = diag\left\{X_C\,\mathbf{J}^{-1},\ 1/X_L\,\mathbf{J}\right\}; \quad \vec{\mathbf{L}} = R\,\mathbf{I}_{2\times 2} \tag{19}$$

The submatrices of junction structure **S** given by (15) are

$$\begin{aligned}
&\vec{\mathbf{S}}_{11} = \begin{bmatrix} \mathbf{0}_{2\times2} & \mathbf{I}_{2\times2} \\ -\mathbf{I}_{2\times2} & \mathbf{0}_{2\times2} \end{bmatrix}; \quad \vec{\mathbf{S}}_{32} = \mathbf{I}_{2\times2}; \\
&\vec{\mathbf{S}}_{13} = \begin{bmatrix} \mathbf{0}_{2\times2} \\ \mathbf{I}_{2\times2} \end{bmatrix}; \quad \vec{\mathbf{S}}_{12} = -\vec{\mathbf{S}}_{21}{}^{T} = \begin{bmatrix} \mathbf{0}_{2\times2} \\ -\mathbf{I}_{2\times2} \end{bmatrix} \\
&\vec{\mathbf{S}}_{22} = \vec{\mathbf{S}}_{23} = \vec{\mathbf{S}}_{31} = \vec{\mathbf{S}}_{33} = \mathbf{0}_{2\times2}
\end{aligned} \tag{20}$$

Finally, (20) is substituted into (16) to obtain the steady-state symbolic function in the complex plane of the output:

$$\begin{bmatrix} e_{6\,\mathrm{Re}} \\ e_{6\,\mathrm{Im}} \end{bmatrix} = \frac{1}{\Delta} \begin{bmatrix} R^2 & -R(X_C - X_L) \\ R(X_C - X_L) & R^2 \end{bmatrix} \begin{bmatrix} e_{1\,\mathrm{Re}} \\ e_{1\,\mathrm{Im}} \end{bmatrix} \tag{21}$$

where $\alpha = R^2 + (X_C - X_L)^2$ In order to verify the proposed methodology, consider the following parameters $u(t) = \sqrt{2}\sin(2\pi f t)$ for the dynamic model and $\vec{\mathbf{u}} = \vec{e}_1 = [1\ \ 0]^T$ for the PhBG model, $C = 0.5\,F$, $R = 10\,\Omega$, $L = 1\,H$, $f = 50\,Hz$. By substituting the numerical parameters into (21) the steady-state value of the output is given by

$$\begin{bmatrix} e_{6\,\mathrm{Re}} \\ e_{6\,\mathrm{Im}} \end{bmatrix} = \begin{bmatrix} 0.0010 \\ -0.0318 \end{bmatrix} \tag{22}$$

It is necessary to obtain the magnitude and the argument of the complex number in (22), so

$$\begin{aligned}
e_6 &= \sqrt{e_{6\,\mathrm{Re}}{}^2 + e_{6\,\mathrm{Im}}{}^2} = 0.0318\,V_{rms} \\
\phi_6 &= \arctan(e_{6\,\mathrm{Im}} / e_{6\,\mathrm{Re}}) = -88.1988^\circ
\end{aligned} \tag{23}$$

As can be seen in Fig. 7, the magnitude value of (23) represents the rms voltage at the output,

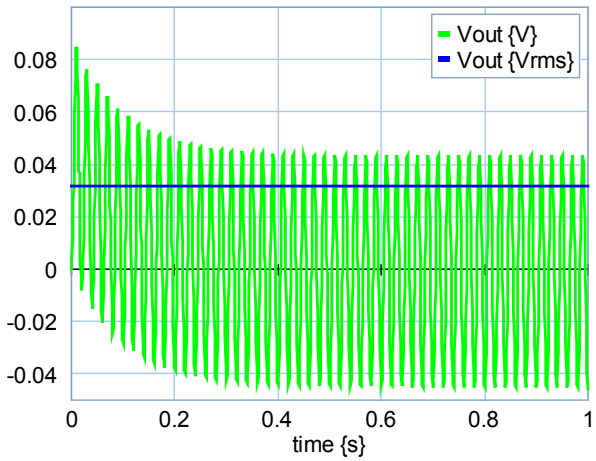

Fig. 7 Comparison between instantaneous output and steady-state value from the PhBG

One advantage of PhBG models arise at this point. As was described before, the impedance depends of the frequency. If the impedances of a PhBG are rewritten as functions of the frequency (see Table 1) is possible to obtain the steady-state response of the output under different frequencies, i.e. Bode, Nichols, and Nyquist plots. Equation (21) may be expressed as

$$\begin{bmatrix} e_{6\,\mathrm{Re}} \\ e_{6\,\mathrm{Im}} \end{bmatrix} = \frac{1}{\Delta} \begin{bmatrix} R^2 & -R(1/\omega C - \omega L) \\ R(1/\omega C - \omega L) & R^2 \end{bmatrix} \begin{bmatrix} e_{1\,\mathrm{Re}} \\ e_{1\,\mathrm{Im}} \end{bmatrix} \tag{24}$$

where $\Delta = R^2 + (1/\omega C - \omega L)^2$. By calculating the output magnitude in decibels, $e_{6\,dB} = 20\log_{10}(e_6)$, and varying the frequency is possible to obtain the Bode magnitude and phase plot of the band pass filter, see Fig. 8.

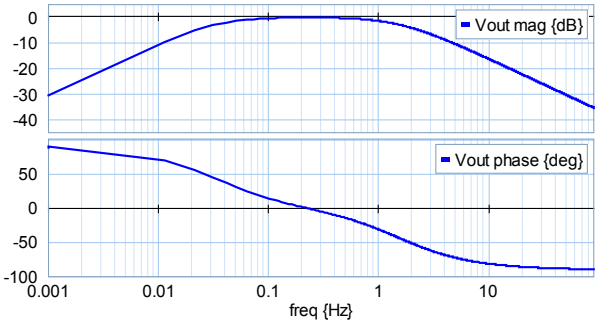

Fig. 8 Bode plot obtained from the PhBG

6. APPLICATION OF PHASOR BOND GRAPHS ON POWER FLOW ANALYSIS

This section deals with the steady-state analysis of an interconnected EPS during normal operation. The system is assumed to be operating under balanced condition and is represented by a single-phase network.

Power flow studies are the backbone of EPS analysis and design. They are necessary for planning, operation, economic scheduling and exchange of power between utilities. The principal information obtained from a power-flow study is the magnitude and phase angle of the voltage at each bus and the real and reactive power flowing in each line (Saadat, 1999).

The system buses are generally classified into three types: i) slack bus, it is taken as reference where the magnitude and phase angle of the voltage are specified; ii) load bus, the magnitude and the phase angle of the bus voltages are unknown; and iii) regulated bus, the real power and the voltage magnitude are specified. Clearly the conditions imposed by the different types of nodes make the problem nonlinear and therefore power-flow equations are commonly solved iteratively using techniques such as the Gauss-Seidel or Newton-Raphson method (Machowski, 2008; Kundur, 1994; Saadat, 1999; El-Harawy, 1995). A detailed description of these algorithms is beyond the scope of this paper but can be found in most textbooks on numerical methods or on power system analysis.

In order to demonstrate the application of PhBG in EPS analysis and to compare results the example illustrated in page 213 of (Saadat, 1999) is used. Fig. 9 shows the one-line diagram of a simple three-bus power system with

generation at bus *a* (slack bus). The magnitude of voltage at bus *a* is adjusted to 1.05 per-unit and 0°. The scheduled loads at buses *b* and *c* are as marked on the diagram. Line impedances and complex loads are marked in per-unit on a 100-MVA base and the line charging susceptances are neglected (Saadat, 1999).

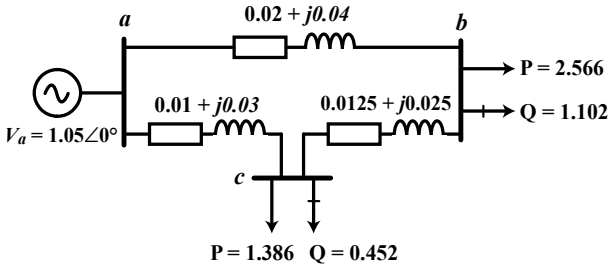

Fig. 9 One-line diagram of a three-bus EPS

The PhBG model of the EPS is shown in Fig. 10.

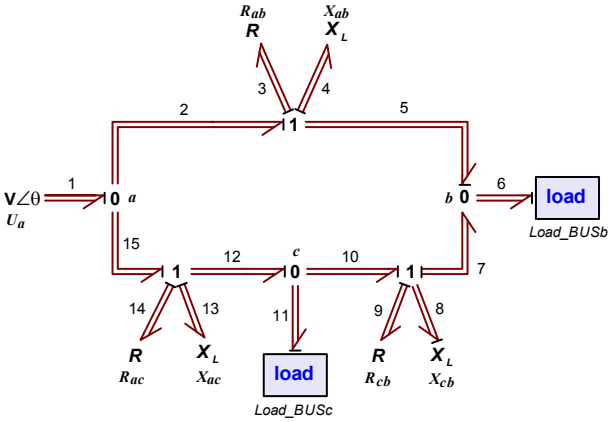

Fig. 10 PhBG model of the three-bus power system

The two load buses are modelled as flow sinks $(\vec{f}_6,\ \vec{f}_{11})$ because of the following reasons:

- it is necessary to determine the phasor values of the voltages at the load buses *b* and *c*, thus voltages at bonds 6 and 11 are defined as outputs,
- if the real and reactive powers are specified, then it is possible to rewrite (8) in the form

$$\begin{bmatrix} I_{\mathrm{Re}} \\ I_{\mathrm{Im}} \end{bmatrix} = \begin{bmatrix} V_{\mathrm{Re}} & V_{\mathrm{Im}} \\ V_{\mathrm{Im}} & -V_{\mathrm{Re}} \end{bmatrix}^{-1} \begin{bmatrix} P \\ Q \end{bmatrix} \tag{25}$$

- the complex voltage may be calculated by iterations.

The causality in the PhBG is propagated through the junction structure following the SCAP. The regular BG model of the power system would have had two elements in derivative causality, in this case (X_{ac}, X_{ab}). Nevertheless, in the PhBG these two elements are simply modeled by the impedance of both inductive reactances. The key vectors are defined as,

$$\omega \mathbf{J}\vec{\mathbf{x}} = \begin{bmatrix} \vec{f}_4 \\ \vec{e}_8 \\ \vec{f}_{13} \end{bmatrix} = \begin{bmatrix} f_{4\,\mathrm{Re}} \\ f_{4\,\mathrm{Im}} \\ e_{8\,\mathrm{Re}} \\ e_{8\,\mathrm{Im}} \\ f_{13\,\mathrm{Re}} \\ f_{13\,\mathrm{Im}} \end{bmatrix};\quad \vec{\mathbf{z}} = \begin{bmatrix} \vec{e}_4 \\ \vec{f}_8 \\ \vec{e}_{13} \end{bmatrix} = \begin{bmatrix} e_{4\,\mathrm{Re}} \\ e_{4\,\mathrm{Im}} \\ f_{8\,\mathrm{Re}} \\ f_{8\,\mathrm{Im}} \\ e_{13\,\mathrm{Re}} \\ e_{13\,\mathrm{Im}} \end{bmatrix}$$

$$\vec{\mathbf{D}}_{in} = \begin{bmatrix} \vec{f}_3 \\ \vec{f}_9 \\ \vec{f}_{14} \end{bmatrix} = \begin{bmatrix} f_{3\,\mathrm{Re}} \\ f_{3\,\mathrm{Im}} \\ f_{9\,\mathrm{Re}} \\ f_{9\,\mathrm{Im}} \\ f_{14\,\mathrm{Re}} \\ f_{14\,\mathrm{Im}} \end{bmatrix};\quad \vec{\mathbf{u}} = \begin{bmatrix} \vec{e}_1 \\ \vec{f}_6 \\ \vec{f}_{11} \end{bmatrix} = \begin{bmatrix} e_{1\,\mathrm{Re}} \\ e_{1\,\mathrm{Im}} \\ f_{6\,\mathrm{Re}} \\ f_{6\,\mathrm{Im}} \\ f_{11\,\mathrm{Re}} \\ f_{11\,\mathrm{Im}} \end{bmatrix} \tag{26}$$

$$\vec{\mathbf{D}}_{out} = \begin{bmatrix} \vec{e}_3 \\ \vec{e}_9 \\ \vec{e}_{14} \end{bmatrix} = \begin{bmatrix} e_{3\,\mathrm{Re}} \\ e_{3\,\mathrm{Im}} \\ e_{9\,\mathrm{Re}} \\ e_{9\,\mathrm{Im}} \\ e_{14\,\mathrm{Re}} \\ e_{14\,\mathrm{Im}} \end{bmatrix};\quad \vec{\mathbf{y}} = \begin{bmatrix} \vec{e}_6 \\ \vec{e}_{11} \end{bmatrix} = \begin{bmatrix} e_{6\,\mathrm{Re}} \\ e_{6\,\mathrm{Im}} \\ e_{11\,\mathrm{Re}} \\ e_{11\,\mathrm{Im}} \end{bmatrix}$$

The constitutive relations of the transmission line elements are

$$\begin{aligned} \vec{\mathbf{F}} &= diag\left\{ X_{ab}\mathbf{J}^{-1},\ \frac{1}{X_{cb}}\mathbf{J},\ X_{ac}\mathbf{J}^{-1} \right\} \\ \vec{\mathbf{L}} &= diag\left\{ R_{ab}\mathbf{I}_{2\times2},\ R_{cb}\mathbf{I}_{2\times2},\ R_{ac}\mathbf{I}_{2\times2} \right\} \end{aligned} \tag{27}$$

For this system, the following junction structure matrices can be constructed:

$$\begin{aligned} \vec{\mathbf{S}}_{11} &= \begin{bmatrix} \mathbf{0}_{2\times2} & -\mathbf{I}_{2\times2} & \mathbf{0}_{2\times2} \\ \mathbf{I}_{2\times2} & \mathbf{0}_{2\times2} & -\mathbf{I}_{2\times2} \\ \mathbf{0}_{2\times2} & \mathbf{I}_{2\times2} & \mathbf{0}_{2\times2} \end{bmatrix} \\ \vec{\mathbf{S}}_{12} &= \begin{bmatrix} \mathbf{0}_{2\times2} & \mathbf{0}_{2\times2} & \mathbf{0}_{2\times2} \\ \mathbf{I}_{2\times2} & -\mathbf{I}_{2\times2} & -\mathbf{I}_{2\times2} \\ \mathbf{0}_{2\times2} & \mathbf{0}_{2\times2} & \mathbf{0}_{2\times2} \end{bmatrix} = -\vec{\mathbf{S}}_{21}{}^{T} \\ \vec{\mathbf{S}}_{13} &= \begin{bmatrix} \mathbf{0}_{2\times2} & \mathbf{I}_{2\times2} & \mathbf{0}_{2\times2} \\ \mathbf{0}_{2\times2} & \mathbf{0}_{2\times2} & \mathbf{0}_{2\times2} \\ \mathbf{0}_{2\times2} & \mathbf{0}_{2\times2} & \mathbf{I}_{2\times2} \end{bmatrix} = \vec{\mathbf{S}}_{23} \\ \vec{\mathbf{S}}_{31} &= \begin{bmatrix} -\mathbf{I}_{2\times2} & \mathbf{0}_{2\times2} & \mathbf{0}_{2\times2} \\ \mathbf{0}_{2\times2} & \mathbf{0}_{2\times2} & -\mathbf{I}_{2\times2} \end{bmatrix} = \vec{\mathbf{S}}_{32} \\ \vec{\mathbf{S}}_{33} &= \begin{bmatrix} \mathbf{I}_{2\times2} & \mathbf{0}_{2\times2} & \mathbf{0}_{2\times2} \\ \mathbf{I}_{2\times2} & \mathbf{0}_{2\times2} & \mathbf{0}_{2\times2} \end{bmatrix} \end{aligned} \tag{28}$$

Substituting (28) into (16), the steady-state symbolic function of the outputs is expressed by

$$\begin{aligned} \vec{\mathbf{y}} &= (\vec{\mathbf{C}}(\vec{\mathbf{F}}^{-1} - \vec{\mathbf{A}})^{-1}\vec{\mathbf{B}} + \vec{\mathbf{D}})\,\vec{\mathbf{u}} \\ &= \frac{1}{\Delta}\begin{bmatrix} 1 & 0 & H_{13} & H_{14} & H_{15} & H_{16} \\ 0 & 1 & H_{23} & H_{24} & H_{25} & H_{26} \\ 1 & 0 & H_{33} & H_{34} & H_{35} & H_{36} \\ 0 & 1 & H_{43} & H_{44} & H_{45} & H_{46} \end{bmatrix}\vec{\mathbf{u}} \end{aligned} \tag{29}$$

where,

$$
\begin{aligned}
H_{13} &= ({r_{ab}}^2 - {X_{ab}}^2)\alpha - r_{ab}(\Delta - 2X_{ab}\beta) \\
H_{14} &= ({r_{ab}}^2 - {X_{ab}}^2)\beta + X_{ab}(\Delta - 2r_{ab}\alpha) \\
H_{15} &= (X_{ab}X_{ac} - r_{ab}r_{ac})\alpha - (r_{ac}X_{ab} + X_{ac}r_{ab})\beta \\
H_{16} &= (r_{ac}X_{ab} + X_{ac}r_{ab})\alpha + (X_{ab}X_{ac} - r_{ab}r_{ac})\beta \\
H_{35} &= ({r_{ac}}^2 - {X_{ac}}^2)\alpha - r_{ac}(\Delta - 2X_{ac}\beta) \\
H_{36} &= ({r_{ac}}^2 - {X_{ac}}^2)\beta + X_{ac}(\Delta - 2r_{ac}\alpha) \\
H_{23} &= -H_{14};\quad H_{24} = H_{13};\quad H_{25} = -H_{16} = H_{43} \\
H_{26} &= H_{15} = H_{44} = H_{33};\quad H_{34} = H_{16} \\
H_{45} &= -H_{36};\quad H_{46} = H_{35}
\end{aligned}
\tag{30}
$$

with $\alpha = r_{ab} + r_{ac} + r_{cb}$, $\beta = X_{ab} + X_{ac} + X_{cb}$, and $\Delta = \alpha^2 + \beta^2$. After substituting the numerical parameters is possible to generate the iterative equation necessary to obtain the node voltage magnitude and angle. Thus,

$$
\vec{\mathbf{y}}^{(k+1)} = \begin{bmatrix} 1 & 0 & -0.011 & 0.023 & -0.005 & 0.013 \\ 0 & 1 & -0.023 & -0.011 & -0.013 & -0.005 \\ 1 & 0 & -0.005 & 0.013 & -0.008 & 0.021 \\ 0 & 1 & -0.013 & -0.005 & -0.021 & -0.008 \end{bmatrix} \vec{\mathbf{u}}^{k} \tag{31}
$$

where,

$$
\vec{\mathbf{y}}^{(k+1)} = \begin{bmatrix} {e_{6\,\mathrm{Re}}}^{(k+1)} \\ {e_{6\,\mathrm{Im}}}^{(k+1)} \\ {e_{11\,\mathrm{Re}}}^{(k+1)} \\ {e_{11\,\mathrm{Im}}}^{(k+1)} \end{bmatrix};\quad \vec{\mathbf{u}}^{k} = \begin{bmatrix} 1.05 \\ 0 \\ {f_{6\,\mathrm{Re}}}^{k} \\ {f_{6\,\mathrm{Im}}}^{k} \\ {f_{11\,\mathrm{Re}}}^{k} \\ {f_{11\,\mathrm{Im}}}^{k} \end{bmatrix}
$$

$$
\begin{bmatrix} {f_{6\,\mathrm{Re}}}^{k} \\ {f_{6\,\mathrm{Im}}}^{k} \end{bmatrix} = \begin{bmatrix} {e_{6\,\mathrm{Re}}}^{k} & {e_{6\,\mathrm{Im}}}^{k} \\ {e_{6\,\mathrm{Im}}}^{k} & -{e_{6\,\mathrm{Re}}}^{k} \end{bmatrix}^{-1} \begin{bmatrix} 2.566 \\ 1.102 \end{bmatrix} \tag{32}
$$

$$
\begin{bmatrix} {f_{11\,\mathrm{Re}}}^{k} \\ {f_{11\,\mathrm{Im}}}^{k} \end{bmatrix} = \begin{bmatrix} {e_{11\,\mathrm{Re}}}^{k} & {e_{11\,\mathrm{Im}}}^{k} \\ {e_{11\,\mathrm{Im}}}^{k} & -{e_{11\,\mathrm{Re}}}^{k} \end{bmatrix}^{-1} \begin{bmatrix} 1.386 \\ 0.452 \end{bmatrix}
$$

with the number of iterations $k = 0, \ldots, n$. The updated voltages immediately replace the previous values in the solution of the subsequent equations. The process is continued until changes in the real and imaginary components of bus voltages between successive iterations are within a specified accuracy, typically $1\text{x}10^{-5}$ to $5\text{x}10^{-5}$ per-unit.

Starting from an initial value of ${e_{6\,\mathrm{Re}}}^{(0)} = 1$, ${e_{6\,\mathrm{Im}}}^{(0)} = 0$ and ${e_{11\,\mathrm{Re}}}^{(0)} = 1$, ${e_{11\,\mathrm{Im}}}^{(0)} = 0$, and after seven iterations the final solution in per-unit is

$$
\begin{bmatrix} e_{6\,\mathrm{Re}} \\ e_{6\,\mathrm{Im}} \\ e_{11\,\mathrm{Re}} \\ e_{11\,\mathrm{Im}} \end{bmatrix} = \begin{bmatrix} 0.98 \\ -0.0599 \\ 1.0 \\ -0.0499 \end{bmatrix} \tag{33}
$$

The solution given by (33) is the same than the one given in (Saadat, 1999). The above result was obtained by both matrix equations in MATLAB® and PhBG model in 20-sim®. Note that, if the reader wish to implement the PhBG model on 20-sim® is necessary to write (32) in the load blocks by means of a delay command.

7. CONCLUSIONS

This study has found that the implementation of 2D multibonds as description of a complex plane successfully may describe a phasor into the BG methodology, which is important because the widespread use of phasors in the analysis of EPS.

One of the significant findings to emerge from this study is that this approach may be implemented in a software tool like, for instance, 20-sim®, which was used in this paper. Thus, it is not only possible to obtain a symbolic function that describes a phasor but also to obtain a numerical simulation. Moreover, the characteristics of BG methodology allow us to maintain the topology of the EPS, and because BG is a form of object-oriented modelling the user may change the complexity of the submodels, e.g. transmission lines models may be easily changed.

When a PhBG model is applied to EPS analysis, the node voltages and angles may be obtained. The usage of delay commands in the simulation allow us to have an iterative PhBG model.

Further research might explore the application of PhBG in other domains where the steady-state is necessary. Other field of research could be the model order reduction in the steady-state. In (Louca, 2014) is proposed to measure the activity (an energy-metric) in steady-state of a quarter car model under different input frequencies. The steady-state activity equations proposed therein may be related to PhBG models.

ACKNOWLEDGMENT

The authors wish to thank CONACYT (Mexican National Council of Science and Technology) and SEP (Mexican Secretary of Public Education) for the funding of this research. We are also immensely grateful to the reviewers for their comments on the draft version of this paper.

REFERENCES

Anderson P.M., Fouad A.A., 2003, Power System Control and Stability. 2nd edition, John Wiley & Sons, USA.

Bonderson L.S., 1975, “Vector Bond Graphs Applied to One-Dimensional Distributed Systems”, J. Dyn. Sys. Meas. Control 97(1), 75-82.

Borutzky W. (Ed.), 2010, Bond Graphs: A Methodology for Modelling Multidisciplinary Dynamic Systems, Springer, London.

Breedveld P.C., 1984a, “A Bond Graph Algorithm to Determine the Equilibrium State of a System”, Journal of the Franklin Institute, vol. 318, No. 2, pp.71-75.

Breedveld P.C., 1984b, “Physical systems theory in terms of bond graphs”, Thesis (PhD), University of Twente, Netherlands, ISBN 90-9000599-4.

Breedveld P.C., 1985, “Multibond graph elements in physical systems theory”, Journal of the Franklin Institute, 319(1/2):1–36.

Chapman S.J., 2005, Electric Machinery Fundamentals, 4th edition, McGraw-Hill, New York.

El-Hawary M.E., 1995, Electrical Power Systems, John Wiley & Sons, New York.

Gonzalez-A G., 2003, “Steady-State Values for a Physical System with Bond Graph Approach”, 9th IEEE International Conference on Methods and Models in Automation and Robotics, pp. 25-28, Miedzyzdroje, Poland.

Karnopp D.C., Margolis D.L., and Rosenberg R.C., 1990, System Dynamics: A Unified Approach. John Wiley & Sons, Inc., New York, USA.

Karnopp D.C., and Rosenberg R.C., 1968, Analysis and Simulation of Multiport Systems - The Bond Graph Approach to Physical System Dynamics. MIT Press, Cambridge, MA.

Kundur P., 1994, Power System Stability and Control. Mc-GrawHill, California, USA.

Kypuros J.A., 2013, System Dynamics and Control with Bond Graph Modeling, Taylor & Francis Group, USA.

Louca L.S., 2014, “Power Conserving Bond Graph Based Modal Representations and Model Reduction of Lumped Parameter Systems”, J. Dyn. Sys., Meas., Control 136(6), 061007 (13 pages).

Machowski J., Bialek J.W., Bumby J.R., 2008, Power System Dynamics: Stability and Control. 2nd edition, John Wiley & Sons, Great Britain.

Paynter H.M., 1961, Analysis and Design of Engineering Systems, The M.I.T. Press, Cambridge, Massachusetts.

Rosenberg R.C., 1971, “State-space formulation for bond-graph models of multiport systems”, J. Dyn. Syst. Meas. Control, 93(1): 35-40.

Saadat H., 1999, Power System Analysis, McGraw-Hill, New York.

Steinmetz C.P., 1893, “Complex Quantities and their use in Electrical Engineering”, Proceedings of the International Electrical Congress, AIEE Proceedings, pp. 33-74.

Veltman A., Pulle D.W.J., and De Doncker R.W., 2007, Fundamentals of Electrical Drives, Springer.